ELSEVIER

Journal of Alloys and Compounds 323–324 (2001) 722–725

Journal of ALLOYS AND COMPOUNDS

www.elsevier.com/locate/jallcom

Efficient $4f^3(^4F_{3/2}) \rightarrow 4f^2 5d$ excited-state absorption in Nd^{3+} doped fluoride crystals

Y. Guyot*, S. Guy, M.F. Joubert

LPCML, UMR 5620 CNRS, Bât 205, Université LYON I, 63 Bd. du 11 Novembre 1918, 69622 Villeurbanne Cedex, France

Abstract

Excited state absorption (ESA) from the $^4F_{3/2}$ metastable level of Nd^{3+} to the $4f^2 5d$ excited configuration has been investigated in $YLiF_4$, $LiLuF_4$ and BaY_2F_8 fluoride crystals doped with Nd^{3+} ions. Efficient ESA cross-sections are obtained around 213 nm and suggest that an up-conversion pumping scheme could be used to reach $4f^2 5d$ for UV tunable source. ESA from the $^4D_{3/2}$ level to the $4f^2 5d$ configuration completes the study. A simple interpretation of the results on observed interconfigurational transitions is given using electric dipole selection rules. © 2001 Elsevier Science B.V. All rights reserved.

Keywords: Fluoride crystals; Neodymium; Optical properties; Excited-state absorption; $4f^2 5d$ Configuration

1. Introduction

$4f^{n-1}5d \rightarrow 4f^n$ interconfigurational transition studies of rare earth-doped crystals are of interest in several optical areas of application such as scintillators or tunable UV solid-state laser materials. In this last research field, to avoid generation of color centers under direct pumping in the $4f^{n-1}5d$ states of rare earth ions, excitation of these states via upconversion processes (which produce population in an excited state whose energy exceeds that of the pump photon) can be considered. With this goal, recent experimental and theoretical studies were done on Pr^{3+}, $Pr^{3+}+Ce^{3+}$ or Nd^{3+} doped crystals [1–6].

The $4f^3$ energy level scheme of Nd^{3+} ions which is almost independent of the host and which was precisely studied in many fluorides, shows three well-known metastable states, $^4F_{3/2}$, $^2P_{3/2}$ and $^4D_{3/2}$. Concerning their use as intermediate states for excited state absorption (ESA) upconversion pumping of $4f^2 5d$ levels, $^4F_{3/2}$ and $^4D_{3/2}$ can be easily achieved by convenient sources such as IR laser diode for the first one and third harmonic generation (355 nm) of Nd:YAG laser for the latter. The location of $4f^2 5d$ levels was studied in many Nd^{3+} doped fluorides and it appears that, in some of them, the successive absorption of two 355-nm photons may lead to population into the lowest Nd^{3+} $4f^2 5d$ band. This is for example the case in the three crystals studied here, Nd:$LiYF_4$, Nd:$LiLuF_4$ and Nd:BaY_2F_8, in which the absorption to the lowest $4f^2 5d$ band starts around 55 000 cm^{-1} [5–9] and in which 355-nm excitation leads to broad emission bands in the UV range (180–280 nm).

In the present contribution, we focus, in these three crystals, on the efficiency of the two following up-conversion excitation mechanisms: $^4I_{9/2} \rightarrow {}^4F_{3/2} \rightarrow 4f^2 5d$ and $^4I_{9/2} \rightarrow {}^4D_{3/2} \rightarrow 4f^2 5d$.

From the theoretical point of view, considering only the spin–orbit coupling (or the free ion) and using the electric dipole selection rules, it is possible to assign one terminal energy level at the bottom of the excited configuration.

2. Experiment

The Nd^{3+} doped fluoride crystals studied here are the sheelites $YLiF_4$:1.6at.%Nd and $LiLuF_4$:0.29 at.%Nd (space group C_{4h}^6) as well as BaY_2F_8:0.4at.%Nd (space group $C_{2/m}$). $4f^2 5d$ levels do not emit in oxides and the garnet $Y_3Al_5O_{12}$:1at.%Nd (space group O_h) is only investigated as a reference for excited state absorption.

Pump-probe techniques are used both for $^4D_{3/2} \rightarrow 4f^2 5d$ excited state excitation (ESE) and $^4F_{3/2} \rightarrow 4f^2 5d$ ESA measurements. In the case of ESE two laser beams are used: the third harmonic generation (355 nm) of a Nd:YAG pump laser, to directly populate the $^4D_{3/2}$ level (pump

*Corresponding author. Tel.: +33-7-244-8000; fax: +33-7-243-1130.
E-mail address: guyot@pcml.univ-lyon1.fr (Y. Guyot).

0925-8388/01/$ – see front matter
PII: S0925-8388(01)01059-3

beam), and the second harmonic generation of a dye laser (giving tunability between 285 and 360 nm) acts as the probe beam. Then the upconverted UV fluorescence around 230 nm ($4f^25d \rightarrow 4f^3\text{-}^2H_{9/2}$) is collected (see details in Refs. [5,6].). To record the ESA spectra from the metastable level $^4F_{3/2}$, a dye laser beam populates this state via levels $^4G_{5/2}$ and $^2G_{7/2}$ followed by rapid multiphonon relaxation. The probe light provided by a CW deuterium lamp (185–300 nm) is very convenient because of the long lifetime (hundreds of microseconds) of the emitting level $^4F_{3/2}$. The light transmitted through the crystal is measured in the presence or not of the pump beam via a Jobin Yvon H20 monochromator and a phonomultiplier Hamamatzu 1477. To correct spectra from photon density, the incident power of the pump laser is checked during the scan.

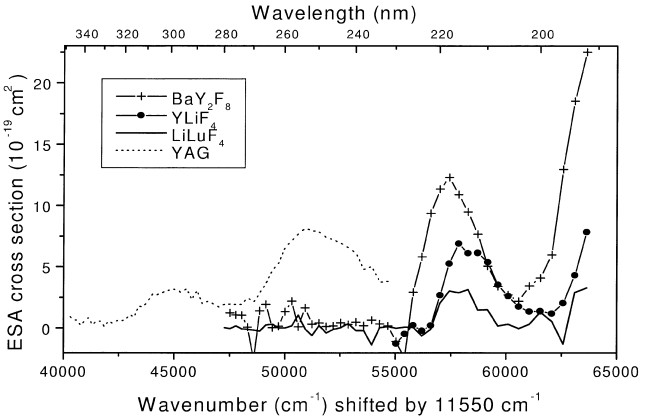

Fig. 2. Excited state absorption spectra of the $^4F_{3/2}$ level in Nd^{3+} doped $LiYF_4$, $LiLuF_4$ and BaY_2F_8 fluoride crystals and YAG oxide. The wave number scale is shifted to $^4F_{3/2}$ energy in order to localize the terminal $4f^25d$ levels.

3. Results

In Fig. 1, the excited state excitation spectra in sigma polarization is compared to ground state excitation spectra of $YLiF_4$. The excitation band is maximum at 330 nm corresponding to a $4f^25d$ level of 58 000 cm^{-1}. So a shift of ~2000 cm^{-1} is obtained for the lowest terminal level of the $^4D_{3/2} \rightarrow 4f^25d$ ESE transition in comparison with the lowest $^4I_{9/2} \rightarrow 4f^25d$ GSA band which is centered at 56 000 cm^{-1}. Measurement, with and without pumping, of the transmitted probe beam at 330 nm permits estimation of the low value (~10^{-20} cm^2) of the maximum ESA cross-section. Note that in π polarization the signal was about twice as weak as that in sigma polarization. ESE spectra recorded with the Nd:$LiLuF_4$ or Nd:BaY_2F_8 crystals are similar indicating very low ESA cross-sections in the 285–360-nm range. We did not succeed in recording ESA spectra from $^4D_{3/2}$ because of the low ESA cross-section.

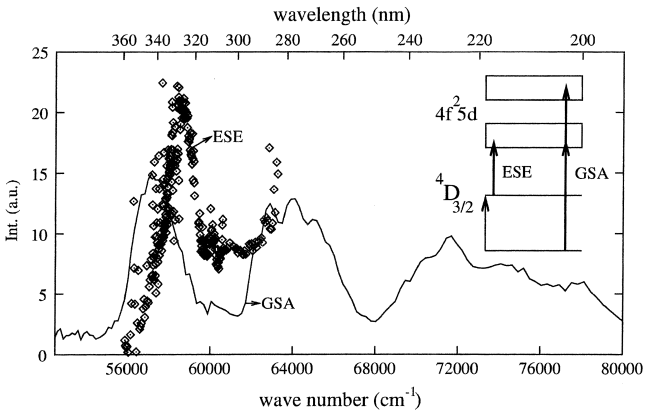

Fig. 1. Excited state excitation (ESE) spectrum from the $^4D_{3/2}$ level to $4f^25d$ (symbols) in $YLiF_4$:Nd. The wave number scale is shifted $\nu = \nu$ ($^4D_{3/2} = 28\,110$ cm^{-1}) + ν (probe) in order to compare with the ground state excitation (GSA) spectrum of the $4f^25d$ excited configuration.

ESA spectra from $^4F_{3/2}$ are shown in Fig. 2. Following the Nd^{3+} concentration and the thickness of each, studied samples from 4 up to 9 mJ are absorbed in the crystals for a spot size of A=~0.053 cm^2. The maximum decrease of transmission varies from 9% in $LiLuF_4$ (5.4-mJ pump absorbed at 590.8 nm for a thickness d=11 mm) to 40% in BaY_2F_8 (3.6-mJ pump absorbed at 590.6 nm, d=4.5 mm). For all samples, the ESA spectra, in the studied range, are formed by two bands separated by a gap of ~8000 cm^{-1}, the strongest band lying at higher energy. Moreover, as in case of $^4D_{3/2} \rightarrow 4f^25d$ transitions, the lowest ESA band is shifted ~2000 cm^{-1} in comparison with the lowest $^4I_{9/2} \rightarrow 4f^25d$ GSA band position. Taking into account the Fresnel reflection, the ESA cross-sections are calculated using the following equation which includes the density of ions in the excited state (the first term of the second part) as well as the delay t between the measurement and the pump pulse

$$\sigma_{\mathrm{ESA}} = \frac{A \exp\left(\frac{t}{\tau}\right)}{P_{\mathrm{abs}}/h\nu_{\mathrm{inc}}} \ln\left(\frac{I_{\mathrm{u}}}{I_{\mathrm{p}}}\right)$$

In this expression, I_u and I_p are the probe intensity when the crystal is unpumped and pumped, respectively, and τ is the lifetime of the $^4F_{3/2}$ level.

The maximum ESA cross-sections are as follows: 0.7×10^{-18} cm^2 in $YLiF_4$ and 0.3×10^{-18} cm^2 in $LiLuF_4$ at 215 nm; and 1.3×10^{-18} and 2.2×10^{-18} cm^2 at 218 and 192 nm, respectively, in BaY_2F_8. For comparison we measured 0.8×10^{-18} cm^2 in YAG at 254 nm. This last value is in the same order as that obtained by Dubinskii and Stolov [10] and is greater than that for Nd:$YAlO_3$ in which 0.2×10^{-18} cm^2 was measured [10].

4. Discussion

The absorption spectrum between three $4f^3$ levels ($^4I_{9/2}$, $^4F_{3/2}$ and $^4D_{3/2}$) and the $4f^25d$ band present fundamental differences (strength and position of the terminal level) depending on the initial level. First, the strength of the transition is high for absorption from the $^4I_{9/2}$ and $^4F_{3/2}$ levels (as expected for allowed electric dipole transition) whereas it is at least two orders of magnitude lower for transitions from the $^4D_{3/2}$ level. Concerning the position of the $4f^25d$ levels it is clear, from the spectra of Figs. 1 and 2, that the terminal levels of the ESA transitions are quite different from those from GSA transitions.

These results and previous UV emission spectra [11,12] show that on the one hand the $4f^25d$ 'bands' are composed of several sublevels and, on the other hand, the transitions between 4f and 4f5d configuration are subject to drastic selection rules. In order to understand these interconfigurational transitions a complete description of $4f^{n-1}5d$ configuration is necessary. Such experimental and theoretical work was recently done in $LiYF_4:Pr^{3+}$ by Laroche et al. [3]. For Nd^{3+} ions the number of levels implicated prevents us following this kind of approach. Following the work of Darenbos on GSA interconfigurational transition [13], we extrapolate the $4f^25d$ levels from those of the free ion: we consider only the free ion and the Russell-Saunders coupling between the three electrons of Nd^{3+}. We assume that the levels of the $4f^25d$ configuration retain in memory a part of the character of the Russell-Saunders coupling even if in the case of crystalline host, the 5d shell is under the influence of the crystal field.

The decomposition of the $4f^25d$ configuration gives rise to 107 ($^{2S+1}$L(5d)) levels, which can be split into 910 ($^{2S+1}L_J$) manifolds. After Ref. [14], the lowest ones are: ^{2}H(5d),^{4}K(5d), which are very close together, then ^{4}I(5d), ^{4}G(5d) and ^{4}H(5d). In this framework, the dipolar electric transitions obey to the following usual selections rules: $\Delta n=1$; $\Delta S=0$; $\Delta L=0, \pm 1$.

Under these rules, the only allowed emission transitions in the UV–visible range from the lowest ^{2}H(5d),^{4}K(5d) levels of the $4f^25d$ configuration are ^{4}K(5d)$\rightarrow ^4I_J$, ^{2}H(5d)$\rightarrow ^2H_{9/2,\ 11/2}$ and ^{2}H(5d)$\rightarrow ^2G_{7/2}$, the other possible terminal levels being too high (above 35 000 cm^{-1}). These transitions correspond well with those observed [11,12]. Concerning the absorption transitions from the ground and the excited states, the terminal levels of the $4f^25d$ configuration should be: $^4I_{9/2}\rightarrow ^4$K(5d), ^{4}I(5d) and ^{4}H(5d); $^4F_{3/2}\rightarrow ^4$G(5d), ^{4}F(5d) and ^{4}D(5d) and finally $^4D_{3/2}\rightarrow ^4$F(5d), ^{4}D(5d) and ^{4}P(5d).

First of all, we can see that the levels involved in the GSA are not involved in the ESA. Then, the observed bands in Fig. 2 at 190 and 213 nm in YLF, and 255 and 300 nm in YAG, are assigned to ($4f^3$) $^4F_{3/2}\rightarrow(4f^25d)^4$G and ($4f^3$) $^4F_{3/2}\rightarrow(4f^25d)^4$F transitions. The last transitions ($4f^3$) $^4F_{3/2}\rightarrow(4f^25d)^4$D was not observed because it is in the VUV range. Knowing the $^4F_{3/2}$ energy, the energy position of the $(4f^25d)^4$F level is determined at 65 000 cm^{-1} in YLF. So, the first allowed ESA band from $^4D_{3/2}$ should be $(4f^3)^4D_{3/2}\rightarrow(4f^25d)^4$F expected around 266 nm. This experiment is under investigation now.

5. Conclusion

Nd^{3+} doped $YLiF_4$, $LiLuF_4$ and BaY_2F_8 fluoride crystals show broad band $4f^25d\rightarrow 4f^3$ UV emissions under 355-nm pumping. However, we measure ESA cross-section less than 10^{-20} cm^2 in the 285–360-nm range of the $^4D_{3/2}\rightarrow 4f^25d$ transition. This is very low and indicates that, unfortunately, upconversion pumping using a 355-nm laser will not be efficient enough for generating tunable $4f^25d\rightarrow 4f^3$ UV radiation. On the other hand, $^4D_{3/2}\rightarrow 4f^25d$ transition electric dipole selection rule considerations suggest efficient upconversion mechanism using 355-nm photons for the first step to promote ions into $^4D_{3/2}$, and higher energy photons (around 266 nm which correspond to the fourth harmonic of Nd:YAG laser) for the second step, $^4D_{3/2}\rightarrow 4f^25d$.

Moreover, excited state absorption spectra using $^4F_{3/2}$ as the intermediate absorbing level show two strong bands around 215 and 190 nm with $Nd:YLiF_4$, $Nd:LiLuF_4$ and $Nd:BaY_2F_8$; and the associated ESA cross-sections are 0.7×10^{-18} and 0.3×10^{-18} cm^2 at 215 nm in $YLiF_4$ and $LiLuF_4$, respectively, and 1.3×10^{-18} and 2.2×10^{-18} cm^2 in BaY_2F_8 at 218 and 192 nm, respectively. This is also interpreted using electric dipole selection rule considerations for the $^4F_{3/2}\rightarrow 4f^25d$ transitions. This suggests efficient upconversion possibilities using convenient sources such as IR laser diode for the first step to promote ions into $^4F_{3/2}$, and higher energy photons (around 213 nm which corresponds to the fifth harmonic of Nd:YAG laser) for the second step, $^4F_{3/2}\rightarrow 4f^25d$.

These new results are extremely promising regarding the potential of Nd-doped fluoride crystals as tunable UV up-conversion lasers using two different but convenient pump beams.

References

[1] S. Nicolas, M. Laroche, S. Girard, R. Moncorgé, Y. Guyot, M.F. Joubert, E. Descroix, A.G. Petrosian, J. Phys. Condens. Matter. 11 (1999) 7937.
[2] M. Laroche, A. Braud, S. Girard, J.L. Doualan, R. Moncorgé, M. Thuau, L.D. Merckle, J. Opt. Soc. Am. B16 (1999) 2269.
[3] M. Laroche, J.L. Doualan, S. Girard, J. Margerie, R. Moncorgé, J. Opt. Soc. Am. B17 (2000) 1291.
[4] V.V. Semashko, M.F. Joubert, E. Descroix, S. Nicolas, R.Y. Abdulsabirov, A.K. Naumov, S.L. Korableva, A.C. Cefalas, Proc. SPIE 4061 (2000) 306.

[5] Y. Guyot, S. Guy, M.F. Joubert. In: C. Jardin (Ed.), Suppl. of 'Le vide: Science technique et applications', Société française du vide (SFV), Paris, ILUM'99, p. 13.
[6] S. Guy, Y. Guyot, A.M. Tkachuk, I.K. Razumova, M.F. Joubert, J. Phys. IV France 10 (2000) Pr8.
[7] J.C. Krupa, M. Queffelec, J. Alloys Comp. 250 (1997) 287.
[8] Z. Kollia, E. Sarantopoulou, A.C. Cefalas, C.A. Nicolaides, A.K. Naumov, V.V. Semashko, R.Y. Abdulsabirov, S.L. Korableva, M.A. Dubinskii, J. Opt. Soc. Am. B12 (1995) 782.
[9] R. Vissert, P. Darenbos, C.W. E van Eijk, A. Meigjerink, H.W. Den Hartos, J. Phys. Condens. Matter. 5 (1993) 8437.
[10] M.A. Dubinskii, A.L. Stolov, Sov. Phys.-Solid State 27 (1985) 1315.
[11] J. Thogersen, J.D. Gill, H.K. Haugen, Opt. Commun. 132 (1996) 83.
[12] M.A. Dubinskii, A.C. Cefalas, E. Sarantopoulou, R.Y. Abdulsabirov, S.L. Korableva, A.K. Naumov, V.V. Semashko, Opt. Commun. 94 (1992) 115.
[13] P. Darenbos, J. Lumin. 87–89 (2000) 970.
[14] J. Sugar, J. Opt. Am. Soc. 53 (1963) 831.